JOURNAL OF NEUROTRAUMA 33:1919–1935 (November 1, 2016)

DOI: 10.1089/neu.2015.4348

Original Articles

Endoplasmic Reticulum Stress and Disrupted Neurogenesis in the Brain Are Associated with Cognitive Impairment and Depressive-Like Behavior after Spinal Cord Injury

Junfang Wu,* Zaorui Zhao,* Alok Kumar, Marta M. Lipinski, David J. Loane, Bogdan A. Stoica, and Alan I. Faden

Abstract

Clinical and experimental studies show that spinal cord injury (SCI) can cause cognitive impairment and depression that can significantly impact outcomes. Thus, identifying mechanisms responsible for these less well-examined, important SCI consequences may provide targets for more effective therapeutic intervention. To determine whether cognitive and depressive-like changes correlate with injury severity, we exposed mice to sham, mild, moderate, or severe SCI using the Infinite Horizon Spinal Cord Impactor and evaluated performance on a variety of neurobehavioral tests that are less dependent on locomotion. Cognitive impairment in Y-maze, novel objective recognition, and step-down fear conditioning tasks were increased in moderate- and severe-injury mice that also displayed depressive-like behavior as quantified in the sucrose preference, tail suspension, and forced swim tests. Bromo-deoxyuridine incorporation with immunohistochemistry revealed that SCI led to a long-term reduction in the number of newly-generated immature neurons in the hippocampal dentate gyrus, accompanied by evidence of greater neuronal endoplasmic reticulum (ER) stress. Stereological analysis demonstrated that moderate/severe SCI reduced neuronal survival and increased the number of activated microglia chronically in the cerebral cortex and hippocampus. The potent microglial activator cysteine-cysteine chemokine ligand 21 (CCL21) was elevated in the brain sites after SCI in association with increased microglial activation. These findings indicate that SCI causes chronic neuroinflammation that contributes to neuronal loss, impaired hippocampal neurogenesis and increased neuronal ER stress in important brain regions associated with cognitive decline and physiological depression. Accumulation of CCL21 in brain may subserve a pathophysiological role in cognitive changes and depression after SCI.

Key words: adult neurogenesis; brain; cognition/depression; ER stress; spinal cord injury

Introduction

Clinical studies show that 40–60% of spinal cord injury (SCI) patients develop long-term cognitive impairments, such as memory span, executive functioning, attention, processing speed, and learning ability.[1–9] The cause of the cognitive deficits in these patients is controversial because of potentially confounding factors, such as concurrent traumatic brain injury (TBI). However, cognitive changes after SCI in patients have been reported without a history or signs of TBI.[3,5,6] After SCI, the incidence rate of depression ranges from 25% and 47%, more than twice that of the general population.[8,10–14] Cognitive/emotional impairments may be detrimental to SCI patients not only in their own right, but because they can compromise rehabilitation and impair recovery.[15,16] Recent experimental studies have reported that SCI in rodent models causes impairment of spatial and retention memory and depressive-like behavior.[17–21]

The endoplasmic reticulum (ER), an important subcellular organelle, serves multiple functions, being important particularly in the synthesis, folding, modification, and transport of proteins.[22,23] Perturbations in ER function, a process named ''ER stress,'' trigger the unfolded protein response designed to restore protein homeostasis. Persistent ER stress or excessive activation eventually initiates cell death. Because of its function in protein folding and transportation, the ER includes a large number of Ca^{2+}-dependent molecular chaperones, such as the 78-kDa glucose regulation protein (GRP78), that has been shown to be related to the survival of neurons.[24] ER dysfunction could be the final common pathway

Department of Anesthesiology and Center for Shock, Trauma and Anesthesiology Research (STAR), University of Maryland School of Medicine, Baltimore, Maryland.
*These authors contributed equally to this work.

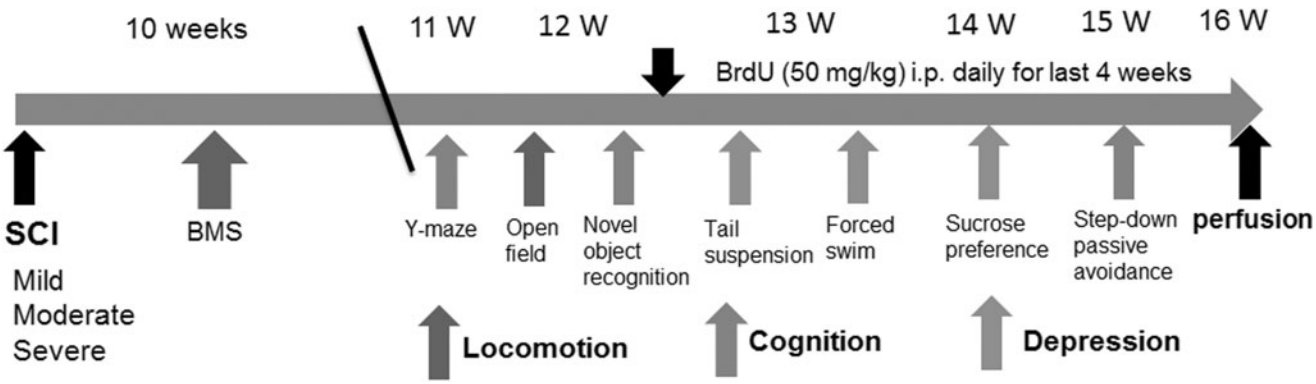

FIG. 1. A timeline of the *in vivo* experimental design. A battery of behavioral tests were evaluated according to the schedule outlined and compared following sham, mild-level (30 kDyne), moderate-level (60 kDyne), or severe-level (100 kDyne) spinal cord injury (SCI). Assessment includes motor function (Basso Mouse Scale [BMS], open field spontaneous activity), cognition (Y-maze, novel object recognition, step-down passive avoidance), and depression (sucrose preference, tail suspension and forced swim tests). ip, intraperitoneal.

for many neurological diseases. Chronic ER stress has been implicated in neuronal disorders causing neurodegeneration and cognitive dysfunction.[25–28] SCI causes increased levels of markers of ER stress, which is a known component of secondary injury.[29–31] However, no studies have examined whether or how SCI can induce ER stress responses in cortex or hippocampus or whether such changes may contribute to neurobehavioral consequences.

Adult hippocampal neurogenesis appears to influence not only memory formation, but also development of depression.[32–34] Remote impaired neurogenesis has been shown after peripheral neuropathy and spinal cord lesions.[18,35–37] However, the relationship between injury severity and the development of hippocampal neurogenesis following SCI is less clear. Brain inflammation can affect neurogenesis and depression. Adult-born hippocampal neurons are sensitive to microglial activation, which can compromise survival and differentiation of newly-formed neurons.[38,39] Increased inflammation in the brain after SCI has been reported not only in pain regulatory areas, such as the brainstem and thalamus, but also in the hippocampus and cerebral cortex.[18,19,21,36,40,41] Moreover, SCI significantly increases M1-like microglial activation genes in the hippocampus, along with changes in M2a-like and M2c-like markers.

In the current study, we evaluated a variety of cognitive and depressive-like behaviors in mice as a function of injury severity after SCI. Neurogenesis, ER stress, and microglial activation in the key regions of the brain were assessed in the same animals.

Methods

Mouse spinal cord contusion and bromo-deoxyuridine injections

C57BL/6J adult male mice (Taconic, Hudson, NY) weighing 20–25 g were anesthetized with isoflurane and received T9 spinal contusions with 30 (mild injury), 60 (moderate injury), or 100 (severe injury) kDyne force using the Infinite Horizon Spinal Cord Impactor (Precision Systems and Instrumentation).[18,42] Bladders were manually expressed twice a day until spontaneous voiding returned. Sham mice received a laminectomy but did not receive spinal cord injuries. Surgical procedures performed on all SCI animals were conducted by the same surgeon and at the same period of time. All surgical procedures and experiments were performed in accordance with the University of Maryland School of Medicine Animal Care and Use Committee.

To determine the impact of SCI on adult neurogenesis and gliogenesis in the brain, as well as to maximize the detection of proliferating cells that would have undergone neuronal/glial differentiation, cumulative *in vivo* labeling of cell proliferation was performed by daily intraperitoneal injections of bromo-deoxyuridine (BrdU; final concentration, 50 mg/kg dissolved in sterile saline; Sigma) for 4 weeks starting 13 weeks post-injury and 4 days per week.

A battery of behavioral tests was conducted by two independent experimenters blinded to injury severity group. The timeline of the experimental design is shown in Figure 1. There were two cohorts of animals that underwent SCI and behavioral testing. Randomization was performed in each study cohort and equal numbers of sham, mild-level, moderate-level, and severe-level injuries were performed on each day of surgery. All conditions were kept consistent throughout the two cohort experiments. The C57BL/6 mice were obtained from the same vendor and were the same age at time of injury. All of the procedures were performed by the same investigators using the same SCI device. In addition, all behavioral tests were performed by the same investigators using the same equipment and room. The number of mice in each group or subgroup is indicated in Table 1.

Table 1. Definition of the Groups

Outcome measures in subgroups/mice # (subgroups, randomly selected)	*Sham*	*Mild SCI*	*Moderate SCI*	*Severe SCI*
BMS	15	15	15	14
OP/NOR/Y-maze	15	15	15	13
TS/FS	15	15	15	12
SP/SDPA	15	15	13	11
IHC for BrdU/DCX/NeuN	8	9	9	9
IHC for BrdU/Iba-1/GFAP	6	5	5	5
IHC for GRP78/DCX	6	7	6	6
IHC for CCL21/NeuN	5	6	5	6
NeuN stereology	5	5	6	5
Iba-1 stereology	5	6	6	6

SCI, spinal cord injury; BMS, Basso Mouse Scale; OP, open field; NOR, novel object recognition; TS, tail suspension; FS, forced swim; SP, sucrose preference; SDPA, step-down passive avoidance; BrdU, bromodeoxyuridine; DCX, doublecortin; NeuN, neuronal nuclei; IHC, immunohistochemistry; Iba-1, ionized calcium binding adaptor molecule 1; GFAP, glial fibrillary acidic protein; GRP78, glucose-regulated protein 78; CCL21, chemokine (C-C motif) ligand 21.

Motor function evaluation

Hindlimb locomotor function was assessed on Day 1 post-injury and weekly thereafter for up to 8 weeks using the Basso Mouse Scale (BMS).[43]The spontaneous locomotor activity was evaluated in the open field[44] and the traveled distance/speed, as well as % of inside zone distance, were recorded by computer-based Any-Maze automated video tracking system (Stoelting Co., Wood Dale, IL).

Cognitive function

Spatial working memory was assessed by Y-maze spontaneous alternation test as previously described.[18] The percentage of alternation is calculated using the following equation: total alternations ×100/(total arm entries - 2). If a mouse scored significantly above 50% alternations (the chance level for choosing the unfamiliar arm), this was indicative of functional working memory. Retention memory was evaluated by novel object recognition (NOR) test as previously reported.[18,44] Time spent with two identical objects was recorded; because mice inherently prefer to explore novel objects, a preference for the novel object (more time than chance [10 sec] spent with the novel object) indicates intact memory for the familiar object. The Step-Down Passive Avoidance (SDPA), conducted as previously reported,[18] evaluated a fear-motivated learning task. Twenty-four hours after conditioning, the latency to step down from the platform was recorded (or when 5 min have elapsed).

Depressive-like behaviors

The sucrose preference (SP) test was used to evaluate interest in seeking a sweet rewarding drink relative to plain water. A diminished preference for the sweetened drink is a sign of anhedonia, indicating depression-like behavior.[45] The SP test was conducted in the home cage as previously described[18] with some modifications. Two inserts were placed in each cage—one with plain water in the normal (back) position and the sweetened water (0.5% saccharine) positioned at the front. After 24 h or 48 h, the water pouches, food, and mice were weighed and recorded. The sucrose preference was calculated by dividing consumption of sweetened water by total consumption of water (sweetened water plus plain water). The food preference also was calculated as a control to demonstrate that mice did not show a place preference.

The tail-suspension (TS) test assesses depression-like behavior in mice and is based on the observation that mice develop an immobile posture when placed in an inescapable hemodynamic stress of being hung by their tail. The duration of immobility was recorded as described.[18,44]

The forced swim (FS) test was performed as previously described.[46,47] Briefly, mice were placed in a transparent plastic cylinder (25 cm high ×20 cm diameter) filled with water (22–23°C; 22 cm in depth). The duration of immobility was recorded throughout the 6 min test period. Immobility was characterized as a lack of any movement.

Immunohistochemistry, image acquisition, and quantification

At 16 weeks after injury, mice were deeply anesthetized and perfused transcardially with 50 mL cold saline, followed by 200 mL of 4% paraformaldehyde (PFA). The brains were removed, post-fixed overnight in PFA, and cryoprotected by immersion in 30% sucrose for 72 h. Serial 30-μm thick coronal sections were cut using a cryostat and stored at −20°C in cryoprotectant solution (25% glycerol, 25% ethylene glycol, and 0.1 M phosphate buffer; pH, 7.4) until use. For BrdU immunohistochemistry, free-floating brain sections were treated with 0.6% H_2O_2 for 30 min to quench endogenous peroxidases. After rinsing in phosphate-buffered saline, sections were incubated in HCl at 37°C for 30 min, followed by washing twice with 0.1 M borate (pH 8.5). Standard fluorescent immunocytochemistry was performed as described previously.[18]

Primary antibodies used in this study include rat anti-BrdU (1:200; AbD Serotec), goat anti-doublecortin (DCX, 1:500; Santa Cruz Biotechnology), mouse anti-NeuN (1:500; Millipore), rabbit anti-ionized calcium binding adaptor molecule 1 (Iba-1, 1:1000; Wako), mouse anti-glial fibrillary acidic protein (GFAP, 1:1000; Dako), rabbit anti-glucose-regulated protein 78 kDa (GRP78, 1:500; Abcam), rabbit anti-chemokine (C-C motif) ligand 21 (CCL21, 1:500; Chemicon). Secondary antibodies used are from Invitrogen: Cy5-conjugated anti-rat, Alexa Fluor 488 goat anti-rabbit, Alexa Fluor 546 goat anti-mouse, Alexa Fluor 633 goat anti-mouse and Alexa Fluor 546 donkey anti-goat. Counterstaining was performed with 4′, 6-diamidino-2-phenylindole (DAPI; 1 μg/mL; Sigma). All immunohistological staining experiments were carried out with appropriate positive control tissue, as well as primary/secondary-only negative controls. Immunofluorescently labeled sections were imaged either using a LEICA (TCS SP5 II, Leica Microsystems Inc., Bannockburn, IL) confocal microscope system (for BrdU/DCX/NeuN, BrdU/Iba-1, and BrdU/GFAP), or using a fluorescence Nikon Ti-E inverted microscope (for GRP78/DCX and CCL21/NeuN). The images were processed using Adobe Photoshop 7.0 software (Adobe Systems, San Jose, CA).

For quantitative image analysis of GRP78/DCX and CCL21/NeuN, images were acquired using a fluorescent Nikon Ti-E inverted microscope, at 20× (CFI Plan APO VC 20× NA 0.75 WD 1 mm) magnification. Exposure times were kept constant for all sections in each experiment. Background for all images was subtracted using Elements. All images were quantified using Elements: nuclei were identified using Spot Detection algorithm based on DAPI staining; cells positive for any of the immunofluorescence markers were identified using Detect Regional Maxima or Detect Peaks algorithms, followed by global thresholding. The number of positive cells was normalized to the total number of cells based on DAPI or NeuN staining. CCL21 intensity was normalized to the total area imaged. All quantifications were performed in the cortex, hippocampus, and thalamus, with $n = 2$–4 images per location from three sections per mouse. The brain sections were chosen between bregma −1.46 mm and bregma −3.16 where hippocampal dentate gyrus (DG) occurs. For each experiment, data from all images from one region in each mouse were summed up and used for final statistical analysis.[31,48] At least 1000–2000 cells were quantified per mouse per area per experiment.

For quantitative image analysis of BrdU/DCX/NeuN, BrdU/Iba-1, and BrdU/GFAP, digital images at 20× magnification were captured from both sides of the DG sub-regions (granular layer [GL] + subgranular zone [SGZ] + hilus), hippocampus or cortex, based on atlas boundaries (from the Franklin and Paxinos mouse atlas, third edition, 2007) and using a confocal laser-scanning microscope ($n = 2$–4 images per location from three sections per mouse for 5–6 mice per group). The brain sections were chosen between bregma −1.46 mm and bregma −3.16 where hippocampal DG occurs. For each experiment, data from all images from one region in each mouse were summed up and used for final statistical analysis.[49,50]

Unbiased stereological quantification of microglial phenotypes and neuronal survival

Brain coronal sections were stained with cresyl-violet and Stereo Investigator software (MBF Biosciences, VT) was used to count the total number of surviving neurons in the cortex, thalamus, as well as Cornu Ammonis (CA) 1, CA2/3, and DG sub-regions of the hippocampus using the optical fractionator method of unbiased stereology as described previously.[18] Every fourth 60-μm section was analyzed beginning from a random start point. The estimated number of surviving neurons in each field was divided by the

volume of the region of interest to obtain the cellular density expressed in cells/mm^3.

Every fourth 60-μm section beginning from a random start point were stained for Iba-1 (1:1000) antibody and 3,3′-diaminobenzidine. The number of the three microglial morphological phenotypes (namely surveillant microglia [ramified], activated microglia [hypertrophic and bushy]) in the cortex and hippocampus was quantified using the optical fractionator method of unbiased stereology with Stereo Investigator software as described previously.[18] Microglial phenotypic classification was based on the length and thickness of the projections, the number of branches and the size of the cell body, as previously described.[51,52] The estimated number of microglia in each phenotypic class was divided by the volume of the region of interest to obtain the cellular density expressed in cells/mm^3. Neurolucida software (MBF Biosciences) was used to create reconstructions of microglia at different stages of activation after injury by tracing the cell bodies and dendrites.[49]

Statistical analysis

Data are presented as means ± standard error of the mean. All statistical analyses were conducted by using the GraphPad Prism Program, Version 3.02 for Windows (GraphPad Software, La Jolla, CA) or SigmaPlot, version 12 (Systat Software, San Jose, CA). BMS was analyzed by two-way analysis of variance (ANOVA) with repeated measures. For multiple comparisons, one-way ANOVA was performed followed by Student's Newman-Keuls *post hoc* test for parametric (normality and equal variance passed) data. Kruskal-Wallis ANOVA based on ranks followed by Dunn's *post hoc* test was used for nonparametric (normality and/or equal variance failed) data. For experiments with only two groups, two-tailed Mann-Whitney rank sum test (nonparametric) or two-tailed unpaired Student's *t*-test was performed. Statistical significance was set at $p \leq 0.05$.

Results

SCI causes severity-dependent impairment of motor/cognitive functions and depressive-like behavior

All mice underwent assessment for hindlimb function in open field locomotion on Day 1 post-injury and weekly thereafter for up to 8 weeks using the BMS. SCI reduced BMS scores in an injury severity–dependent manner (Fig. 2A). Repeated measures two-way ANOVA showed a significant effect of injury severity ($p < 0.001$) and Student-Newman-Keuls *post hoc* analysis demonstrated significant differences between the injured and sham groups ($p < 0.001$, $n = 14$–15/group). There was separation among the mildly-, moderately-, and severely-injured groups from Day 14 through to Day 56. Determination of spontaneous locomotor activity at 12 weeks post-injury using the open-field test showed that moderate ($n = 15$, $p < 0.01$) or severe ($n = 13$, $p < 0.001$) SCI resulted in a significantly reduced distance traveled and walking speed, compared with sham mice ($n = 15$; Fig. 2B). In addition, significant differences were observed between the mildly- and moderately-injured groups ($p < 0.01$) and between the moderately- and severely-injured groups ($p < 0.01$). Moderate/severe injury mice displayed decreased percentages of inside zone distance indicating severity-dependent increased anxiety-like behavior (Fig. 2B).

To investigate the effect of injury severity on learning and memory impairments after SCI, we performed a variety of neurobehavioral tests that are less dependent on locomotion. Non-spatial retention memory was evaluated by a NOR test at 12 weeks post-injury. During training (sample phase), all mice spent equal time with the two identical objects (Fig. 3A, left panel). Sham or mild SCI mice spent more time than chance (10 sec) with the novel object 24 h after training, indicating intact memory (Fig. 3A, right panel), whereas moderate/severe injury mice spent less time than chance. One-way ANOVA analysis revealed that the moderate/severe SCI mice spent significantly reduced time with the novel object, compared with the sham-injured group ($p < 0.001$). No significant differences were observed between the sham and mild SCI groups.

Next, spatial working memory was assessed by the Y-maze spontaneous alternation test at 11 weeks after SCI. Sham or mild SCI mice showed approximately 70% spontaneous alteration, indicative of functional working memory (Fig. 3B). Moderate or severe SCI caused a significant reduction of spontaneous alteration, compared with sham animals. To determine the long-term effect of injury severity on what is believed to be spatial and emotional motivations, the step-down fear avoidance test was conducted at 15 weeks post-injury. This is a fear-motivated learning task that is not dependent on motor function. During step-down fear conditioning trials, all mice displayed similar short retention times before stepping down onto the platform and receiving a shock. During testing for memory of the aversive experiences 24 h later, SCI resulted in reduced latency to step down from the platform in an injury-severity dependent manner (Fig. 3C). Severely injured mice showed significantly reduced latency to step-down, compared with sham mice ($p < 0.05$).

A battery of established tests was used to assess depressive-like behavior in a mouse contusion model of SCI. To reduce the potential confounding effects of motor deficits, water/food motivations were evaluated using the sucrose preference test at 14 weeks after SCI. SCI mice showed significantly reduced sweet water consumption without a change in food consumption, indicating depression-like behavior (Fig. 4A). Immobility in tail-suspension and forced swim tests is interpreted as a symptom of learned helplessness and characteristic of depression in rodent subjects. As shown in Figure 4B and 4C, the sham-injured mice revealed an immobility time of approximately 100 sec. No differences were observed between the sham and mild SCI groups. However, moderate or severe SCI at 13 weeks post-injury resulted in significant increases in immobility times, compared with the sham group ($p < 0.05$, $p < 0.01$, $p < 0.001$, respectively; $n = 13$–15/group).

Collectively, these data show that SCI mice displayed deficits in motor function in an injury severity–dependent manner. Moderately/severely injured mice performed poorly in the Y-maze, NOR, SDPA, SP, TS, and FS tests, indicating impaired cognitive functions and depression-like behavior. In particular, no significant differences were observed between the moderate- and severely-injured groups in these tests.

SCI disrupts neurogenesis in dentate gyrus of the hippocampus

To investigate whether a spinal cord distant lesion impacts hippocampal neurogenesis that is believed to contribute to memory formation and depression,[32–34] mice received BrdU injections between Weeks 13 and 16 post-injury, and brain sections were double-labeled with antibodies specific for BrdU and newly-generated immature neurons (DCX) or mature neurons (NeuN). BrdU positive cells, as well as cells co-labeled with DCX and NeuN, were quantified in the hippocampal DG sub-regions (including GL, SGZ, and hilus) at 16 weeks after SCI (Fig. 5A). The total number of BrdU$^+$ cells was reduced by 16% ($n = 8$), 29%

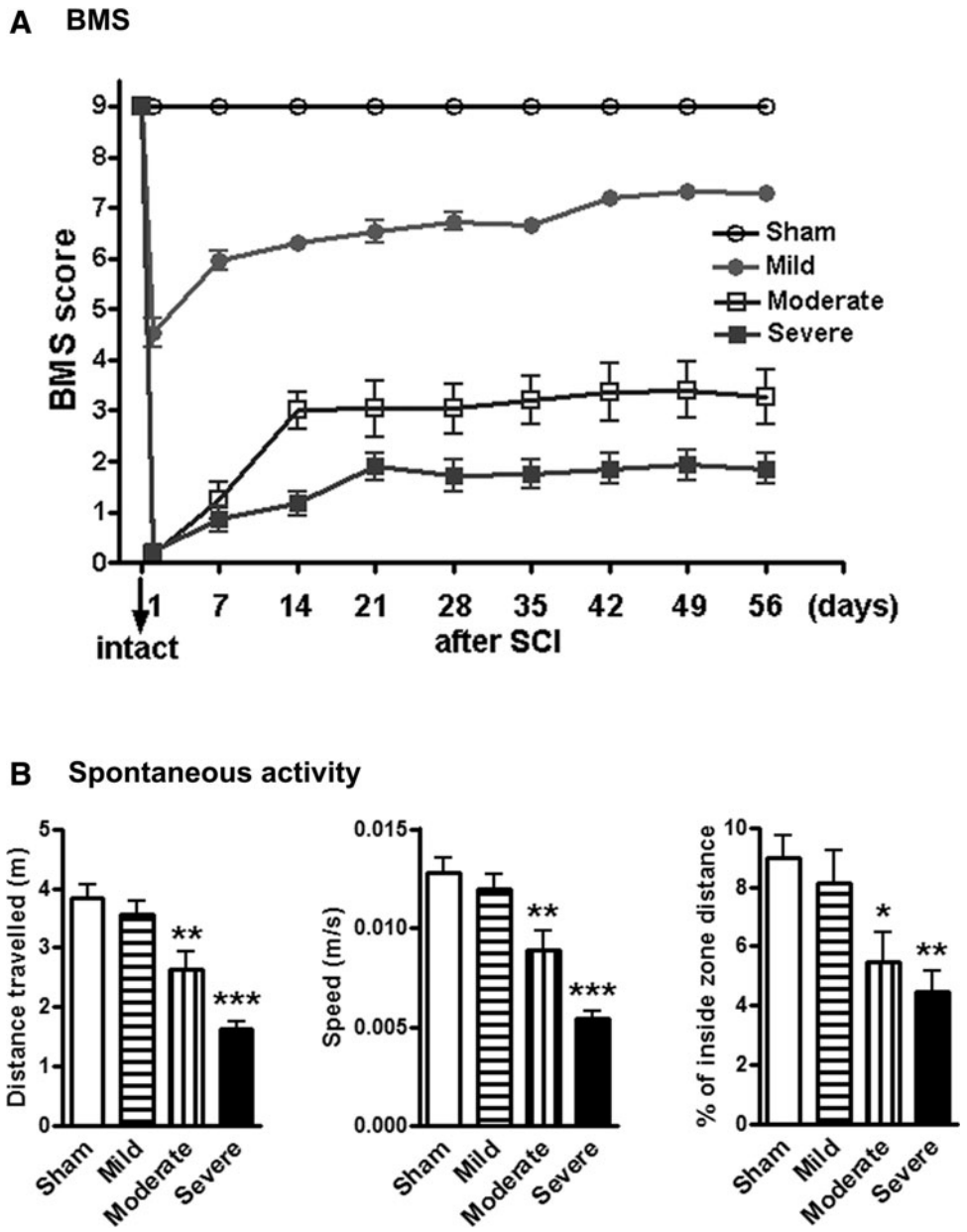

FIG. 2. Spinal cord injury (SCI) causes impairments of motor function in an injury-severity dependent manner. **(A)** Hindlimb locomotor function was evaluated using the Basso Mouse Scale (BMS) score. SCI reduced BMS scores in an injury-severity dependent manner. **(B)** Determination of spontaneous locomotor activity. SCI resulted in a significant reduced distance traveled (left panel), walking speed (middle panel), and percent of inside zone distance (right panel), compared with sham mice.

($n=9$), and 31% ($n=9$), respectively, in the mild, moderate, and severe SCI groups, compared with the sham-operated group ($n=8$; Fig. 5B). Moderate/severe SCI resulted in significant reduction in the number of newly-generated $BrdU^+$ cells ($p<0.05$). Immature neurons stained by DCX were significantly decreased by 33% ($p<0.01, n=9$), 52% ($p<0.001, n=9$), and 42% ($p<0.001; n=9$), respectively, in the mild, moderate and severe SCI groups, compared with sham mice ($n=8$; Fig. 5C). Figure 5D and 5E show representative immunohistochemical images for BrdU and DCX in the DG in sham, mild, moderate, and severe SCI. The number of co-localized $BrdU^+/DCX^+$ and $BrdU^+/NeuN^+$ cells showed a significant decrease in newly-generated immature (Fig. 5F) and mature neurons (Fig. 5H) after mild, moderate, and severe SCI. The percentage of newly-generated immature neurons ($BrdU^+/DCX^+$) in total number of $BrdU^+$ nuclei was reduced but did not reach the significance (Fig. 5G), while the proportion of newly-generated mature neurons ($BrdU^+/NeuN^+$) among the total number of $BrdU^+$ nuclei was significantly decreased in the moderate and severe SCI groups, compared with sham mice (Fig. 5I). Thus, SCI causes long-term reduction in the number of newly-generated neurons and also alters the ability to differentiate from immature neurons to the neuronal lineage in the hippocampal DG region.

SCI results in neuronal ER stress and neurodegeneration in key-regions of the brain

To directly evaluate the possibility that SCI increases neuronal ER stress in the brain, which is implicated as a significant

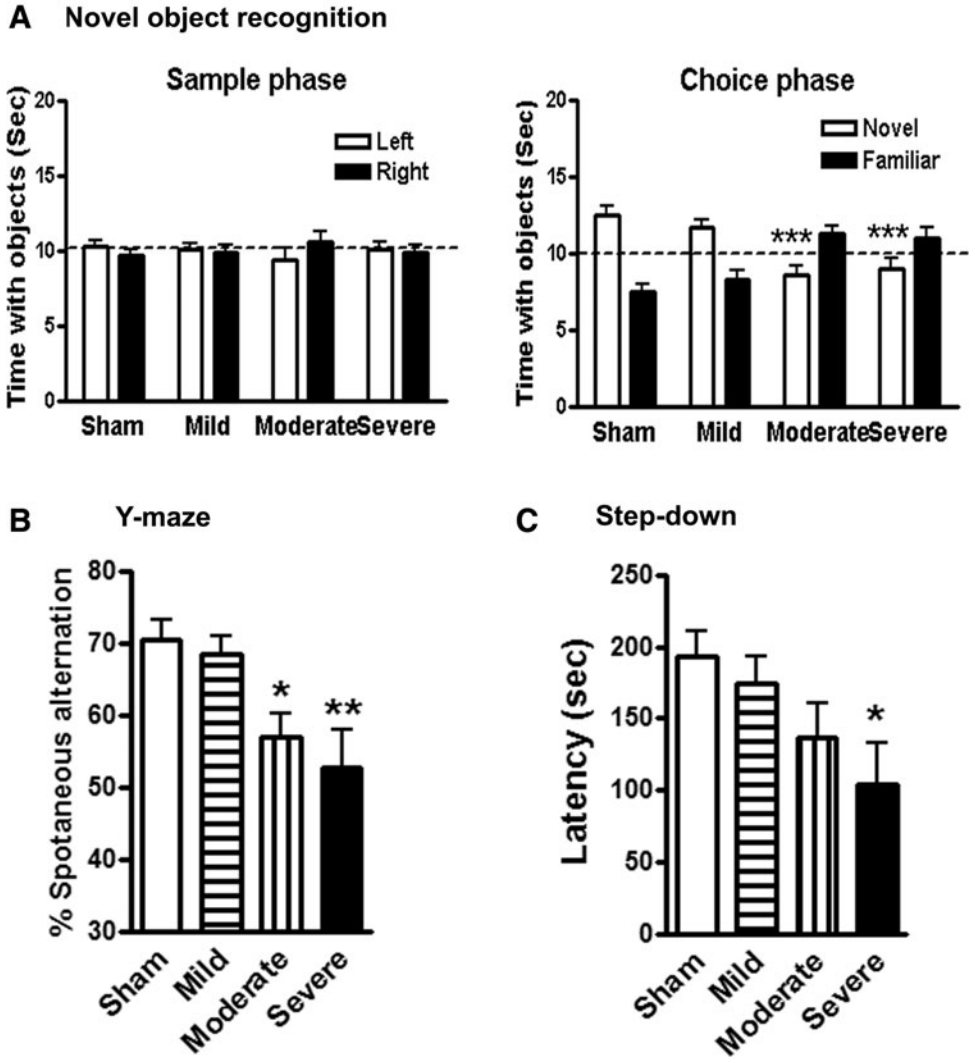

FIG. 3. Spinal cord injury (SCI) causes learning and memory impairments. **(A)** Novel object recognition test. Mice from sham or mild groups spent more time than chance (10 sec) with the novel object 24 h after training (sample phase), indicating intact memory. SCI mice with moderate or severe injury spent significantly less time with the novel object. **(B)** Y-maze spontaneous alteration test. Sham mice showed approximately 70% spontaneous alteration, indicative of functional working memory. Moderate or severe SCI caused a significant reduction of spontaneous alteration, compared with sham animals. **(C)** Step-down passive avoidance (SDPA) test. During SDPA conditioning trials, all groups exhibited similar short retention times before stepping down onto the platform and receiving a shock. During testing for memory of the aversive experiences 24 h later, SCI mice showed significantly reduced latency to step-down from the platform, compared with sham mice. $n = 11$–15/group. $^{*}p < 0.05$, $^{**}p < 0.01$, $^{***}p < 0.001$ vs. sham group.

contributor to neurodegeneration and cognitive dysfunction,[27,28] we examined the expression of ER stress marker, the 78 kDa glucose-regulated protein (GRP78), in the brain at 16 weeks after SCI. Quantitative image analysis revealed that GRP78^{+} cells were significantly increased in the cortex, hippocampus, and thalamus in an injury severity–dependent manner (Fig. 6A–C; $p < 0.01$ mild vs. moderate in cortex; $p < 0.05$ mild vs. moderate in hippo; $p < 0.01$ mild vs. moderate, and moderate vs. severe in cortex). Representative immunofluorescent images for GRP78 were shown in the key brain regions from sham, mild, moderate, and severe SCI mice (Fig. 6D). The majority of positive cells had neuronal morphology. Further, double-labeled GRP78 with DCX were counted in the hippocampal DG. Moderate/severe SCI significantly increased the number of GRP78^{+}/DCX^{+} cells (Fig. 6E), suggesting that proliferating immature neurons underwent ER stress. Figure 4F showed a representative image for GRP78^{+}/DCX^{+} cells from moderate SCI mice. High-magnification image of GRP78 (red) co-labeling with DCX (green; Fig. 6G) is shown in the insert in Figure 6F.

Unbiased stereological assessment of neuronal density was performed on a cresyl-violet–stained section in the cortex, thalamus, and CA1, CA2/3, and DG sub-regions of hippocampus. The survival neurons were significantly reduced in both the moderate and severe SCI groups (Fig. 7A–E). The survival neurons in the DG a trend toward decrease, though no statistically significant difference was found (Fig. 7F).

SCI alters microglial morphology in the brain

To determine whether disrupted neurogenesis and neurodegeneration associated with impaired cognition/depression were the result of increased inflammation, we performed unbiased stereological

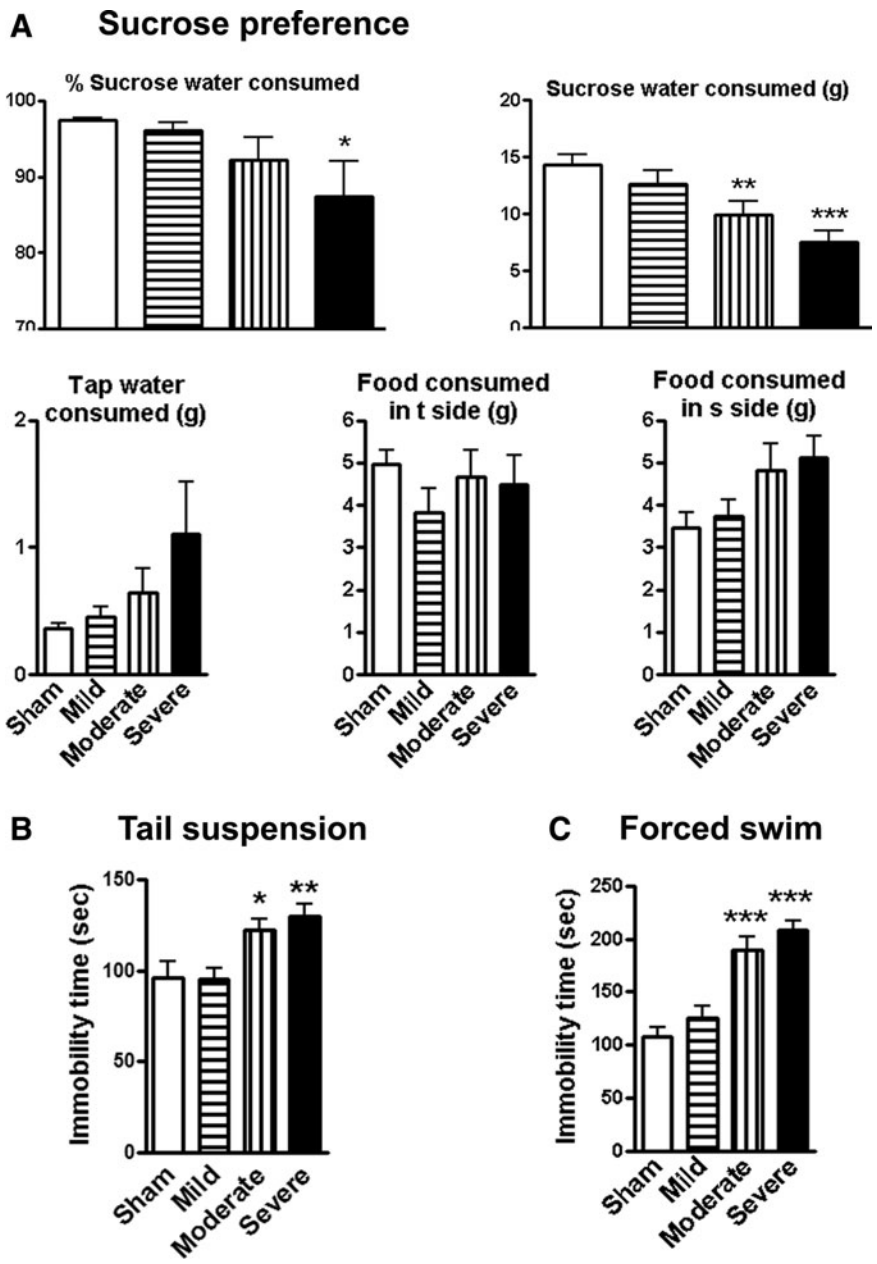

FIG. 4. Spinal cord injury (SCI) mice display depressive-like behavior. **(A)** Sucrose preference (SP) test. The SP is calculated by divided consumption of sweetened water (0.5% saccharine) by total consumption of water (sweetened water plus plain water). The food preference also is calculated as a control to demonstrate that mice do not show a place preference. SCI mice showed significantly reduced sweet water consumption without a change in food consumption. **(B)** Tail-suspension test: SCI resulted in significantly increases in immobility times, compared with Sham group. **(C)** Forced swim test: Rodent develops depression-like status demonstrated by immobility in unescapable water cylinder. Depression-like effect is increased with the severity. $n = 11–15$/group. $^{*}p < 0.05$, $^{**}p < 0.01$, $^{***}p < 0.001$ vs. sham group.

assessment to examine microglial cell numbers and activated forms in the cortex and hippocampus after SCI. Representative images and reconstructions (Neurolucida) of the surveillant (ramified, small cell body with elongated and thin projections) and activated (hypertrophic, large cell body with shorter and thicker projections) microglia were presented (Fig. 8A, 8B). Among activated microglia, hypertrophic phenotypes predominated, whereas bushy microglia (enlarged cell body with multiple short processes that form thick bundles) were rarely seen. No significant differences were observed in the number of total microglia across the groups (Fig. 8C, 8D). However, 16 weeks after moderate/severe SCI, there were significantly increased numbers of microglia displaying the activated phenotype and reduced ramified phenotypes in both the hippocampus and cerebral cortex of SCI mice, compared with sham mice (Fig. 8C, 8D).

To gain further insights into glial proliferation, BrdU labeling Iba-1^{+} microglia or $GFAP^{+}$ astrocytes also were analyzed using the same animal groups for neurogenesis. Figure 9A–B illustrated the hippocampal and cerebral cortical anatomical regions used for image analysis. Neither number of co-localized $BrdU^{+}$/Iba-1^{+} nor

$BrdU^+/GFAP^+$ cells in the hippocampus (Fig. 9C, 9D) and cortex (Fig. 9E. 9F) were changed among the SCI groups.

Together, these data suggest that moderate/severe thoracic SCI triggers microglia activation in the brain without affecting gliogenesis.

CCL21 accumulation in the brain following SCI

The neuroimmune modulator CCL21 was reported to be upregulated in the ventro-posteriolateral nucleus and posterior nucleus of the thalamus after SCI which triggers thalamic microglial activation in association with hyperesthesia.[49,53] More recently, CCL21 signaling was found increased in neuronal cell bodies and parenchyma within both the hippocampus and cortex at 7 days after SCI.[19] Here, we examined CCL21 immunoreactivity in key brain regions from sham, mild, moderate, and severe SCI mice at 16 weeks post-injury. Quantification of pixel intensity for CCL21 revealed significant increases in the cortex, hippocampus, and thalamus in all injured groups (Fig. 10A–C). However, no significant differences were observed in the CCL21 expression across the injured groups. Representative immunofluorescent images for CCL21 were shown in the brain regions from sham, mild, moderate, and severe SCI mice (Fig. 10D). Some of positive cells had neuronal morphology. Further, double-labeled CCL21 with NeuN were counted in these regions. SCI significantly increased the number of $CCL21^+/NeuN^+$ cells (Fig. 10E–G), suggesting that SCI triggers CCL21 accumulation in the neurons in the brains.

Discussion

Using a battery of neurobehavioral tests that are less dependent on locomotion, this study shows that cognitive impairment and depressive-like behavior increase in moderate and severe SCI animals. SCI caused a chronic reduction of BrdU incorporation, as well as immature neurons in the hippocampal DG region. Increased neuronal ER stress response and CCL21 accumulation occurred in selected brain regions associated with elevated numbers of reactive microglia and increased gene expression levels for markers of M1-type microglia. Stereological analysis demonstrated reduced neuronal counts in the cortex, hippocampus, and thalamus in moderate and severe SCI animals.

Cognitive impairment and depression have been reported in humans, as well as in rodents, following SCI.[17–20] However, a direct relationship between injury severity and associated cognitive deficits or depression has not been established. Importantly, for an SCI model, the characterization of behaviors for cognition and depression should not depend on motor function. The Y-maze, NOR, and SDPA tests used in the present study are less dependent on locomotion, reflecting both frontal cortical and hippocampal function, as well as a fear-motivated learning task. These tests showed increased deficits as a function of severity of injury.

The SP, TS, and FS tests are commonly used to measure depression-like symptoms in rodents. In SCI model, Leudtke and colleagues determined that approximately 35–39% of rats with a moderate contusion display characteristics of depression, including decreased anhedonia and social exploration, as well as increased immobility.[20] The latter symptom on the FS test can be reversed by an antidepressant fluoxetine with a dose that has been shown to be subthreshold for increasing motor activity. In the present study, moderately- or severely-injured mice displayed depressive-like behavior, with no significant differences observed between these groups. Despite significant differences in locomotor function between the moderate- and severe-injury groups, injury severity did not affect performance on the tests of cognition and depression, suggesting that these ''non-motor'' tasks are to a significant degree independent of locomotor impairments. This is in agreement with prior reports in rat SCI.[20,21] Whereas the SDPA was independent of motor activity, pain sensation changes in injured mice may affect this test. SCI-mediated chronic pain could potentially contribute to depression.

We and others have reported[42,54–56] that mice with a mild or moderate contusion SCI developed significant tactile allodynia, compared with naïve animals; however, only severe injury mice showed impairment in the SDPA test. Thus, the behaviors observed in the present study appear to be valid measures of cognition and depression in the rodent model of SCI. Although we acknowledge that in certain cases the interpretation of cognitive tests may be confounded by motor deficits, our data indicate that these factors do not play a major role in our model. Maldonado-Bouchard and colleagues [21] have reported in a rat SCI model that mild injury also causes depression- and/or anxiety-like signs. However, mild SCI mice in the present study did not show significant impairment of cognition or depression.

Adult hippocampal neurogenesis, a form of neuronal plasticity, is known to be important in memory formation and maintenance. Numerous groups have reported suppressed hippocampal neurogenesis in depressed subjects and increased adult-born hippocampal neurons with antidepressive drug actions.[34,57–60] Remote hippocampal neurogenesis also is inhibited in some chronic pain models evoked by peripheral nerve injury that is associated with depression.[35,37] Assessments of neurogenesis in the brain after SCI have been controversial. Significant long-term reduction of neurogenesis in the hippocampal SGZ has been reported at 90 days after a cervical spinal cord hemisection injury in adult rats,[36] whereas Franz and colleagues reported no alteration of neurogenesis in the brain at 42 days after rats thoracic moderate contusion.[61] We reported reduced numbers of DCX-labeled immature neurons in the hippocampal SGZ area at 12 weeks after mouse thoracic

FIG. 5. The hippocampal neurogenesis is impaired following spinal cord injury (SCI). **(A)** Approximate positions of the hippocampal anatomical structures are shown in an atlas overlay. The insert shows the dentate gyrus (DG) area for digital images captured at 20× magnification, which included granular layer (GL), subgranular zone (SGZ), and hilus. **(B)** Proliferating cells stained by bromodeoxyuridine (BrdU) were significantly decreased in the moderate and severe SCI groups, compared with sham mice. $*p < 0.05$ vs. sham group. $n = 8–9$. **(C)** Immature neurons stained by doublecortin (DCX) were significantly decreased in the mild, moderate, and severe SCI groups, compared with sham-operated group. $**p < 0.01$, $***p < 0.001$ vs. sham group. $n = 8–9$. (**D** and **E**) Representative images showed BrdU+ and DCX+ cells along with nuclear staining (4',6-diamidino-2-phenylindole, blue) in the hippocampal DG sub-region in sham, mild, moderate, and severe SCI mice. Scale bar = 250 μm. (**F–I**) Number of co-localized BrdU+/DCX+ and BrdU+/NeuN+ cells showed a significant decrease in proliferating immature (F) and mature (H) neurons in mice with mild, moderate, and severe SCI. The percentage of BrdU+/DCX+ in total proliferating cells (BrdU+) did not reach the significance while the percentage of proliferating mature neurons (BrdU+/NeuN+) was significantly decreased in the moderate and severe SCI groups, compared with the sham-operated group. $*p < 0.05$, $**p < 0.01$, $***p < 0.001$ vs. sham group. $n = 8–9$. Color image is available online at www.liebertpub.com/neu

SCI.[18] In the present study, using BrdU labeling, we detected robust down-regulation of neurogenesis at 16 weeks post-injury, including decreased cell proliferation and newly-generated immature neurons, as well as neuronal differentiation. The divergent findings may be explained by the different lesion paradigms or time windows after injury. These alterations are correlated with progressive inflammation in the brain after SCI.[18] Therefore, our data suggest that the SGZ is sensitive to the deleterious effect of SCI, and suppressed hippocampal neurogenesis after SCI may contribute to memory impairment and depression.

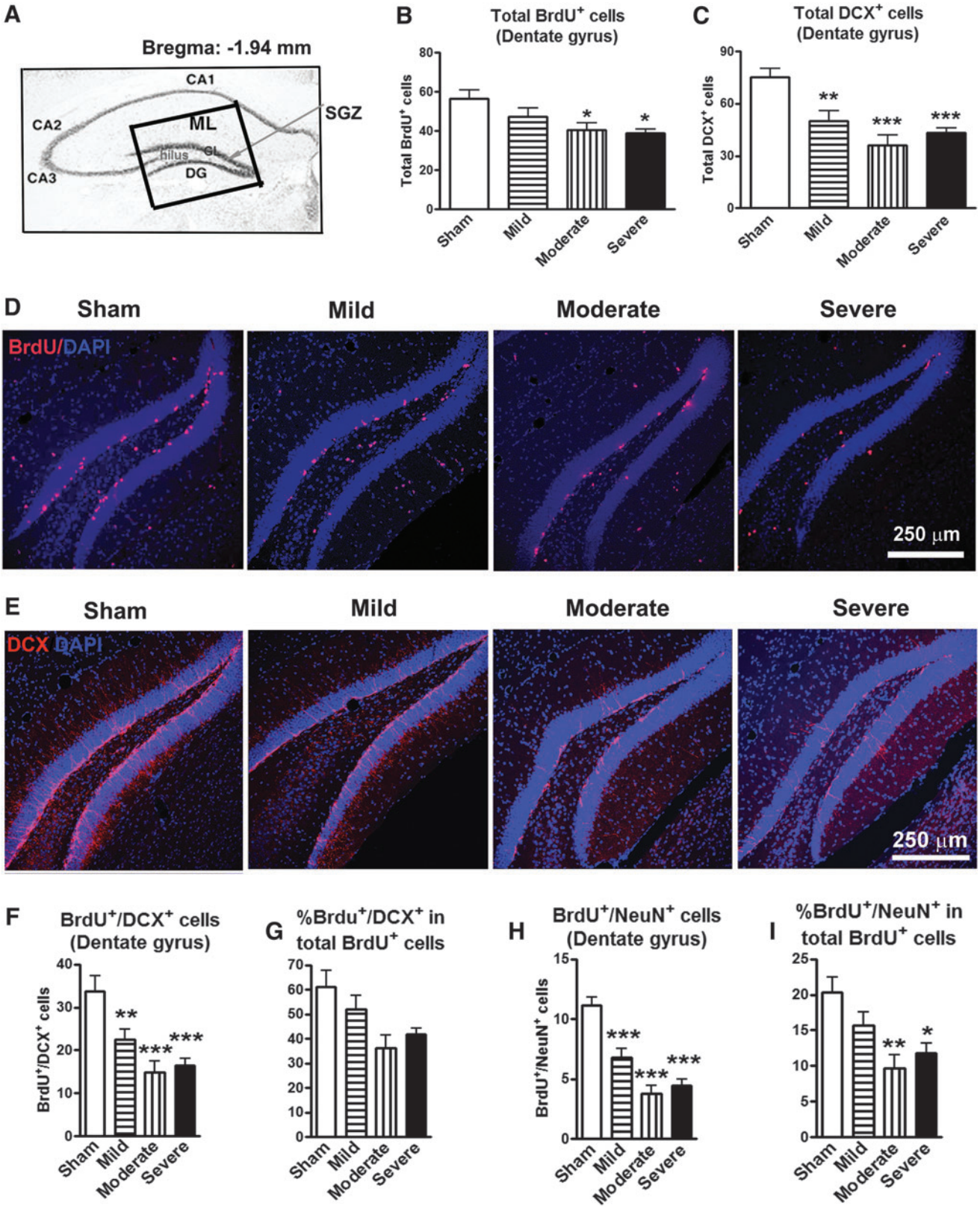

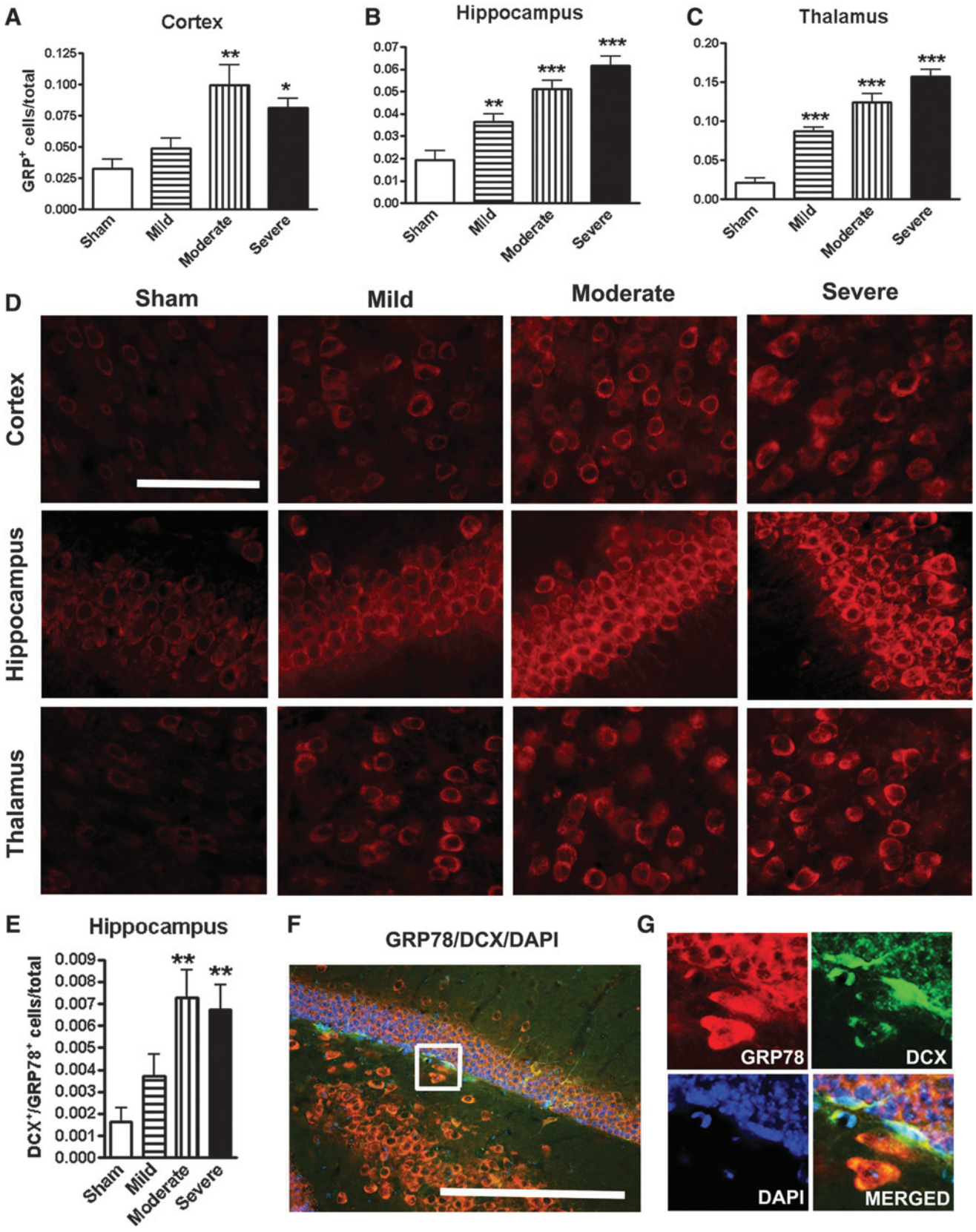

FIG. 6. Spinal cord injury (SCI) increases neuronal endoplasmic reticulum (ER) stress in the brain. (**A–C**) Quantification of ER stress marker 78-kDa glucose regulation protein (GRP78)+ cells showed significantly increased in the cortex, hippocampus, and thalamus in an injury severity–dependent manner. **(D)** Representative images of immunohistochemistry staining for GRP78 in the key brain regions from sham, mild, moderate, and severe SCI animals. **(E)** Quantification of GRP78+/ doublecortin (DCX)+ double-labeling cells in hippocampal DG. **(F)** A representative image for GRP78+/DCX+ cells from moderate SCI mice. **(G)** High-magnification image of GRP78 co-labeling with DCX from the insert in F. All scale bars are 50 μm. *p < 0.05, **$p < 0.01$, ***$p < 0.001$ vs. sham group. $n = 6$–7. Color image is available online at www.liebertpub.com/neu

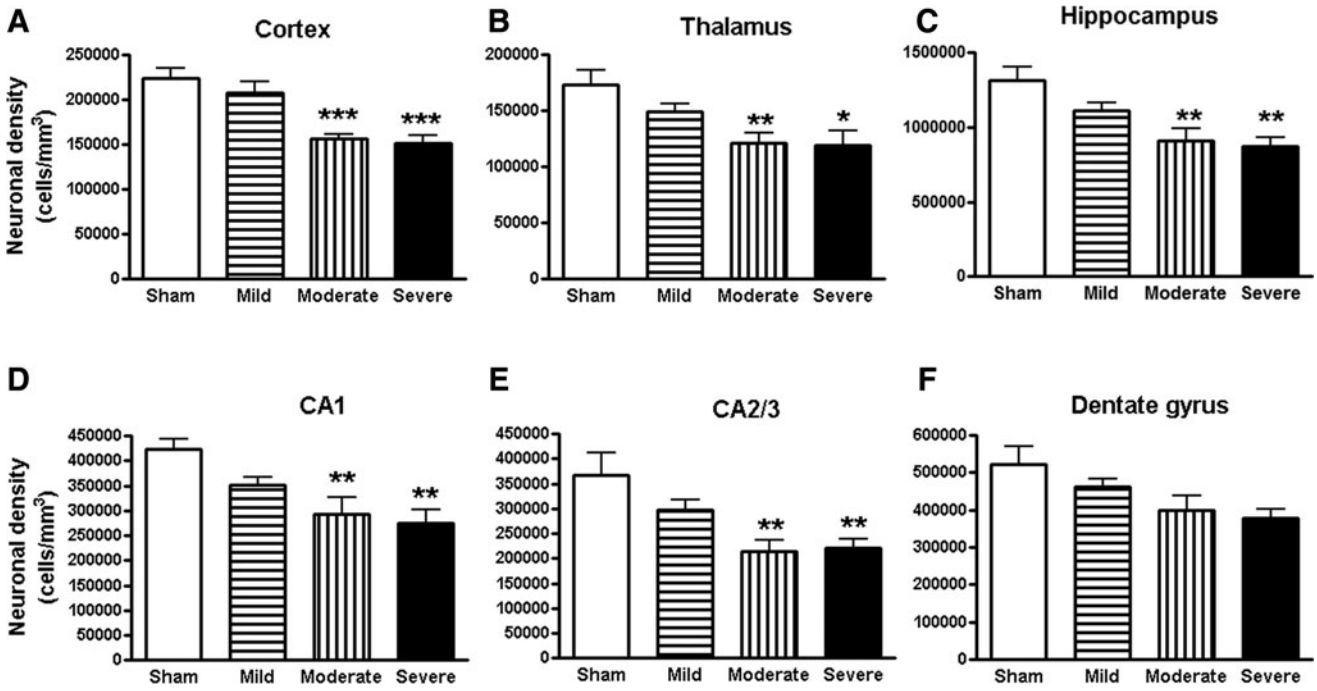

FIG. 7. Spinal cord injury (SCI) mediated chronic neurodegeneration in the brain. Unbiased stereological assessment of neuronal density was performed on cresyl-violet–stained section in the cortex, thalamus, and CA1, CA2/3, and dentate gyrus sub-regions of hippocampus. Surviving neurons were significantly reduced in cortex **(A)**, thalamus **(B)**, hippocampus **(C)**, and CA1 **(D)**, CA2/3 **(E)** sub-regions of hippocampus in both the moderate and severe SCI groups. The survival neurons in the DG **(F)** were not significantly different. $*p<0.05$, $**p<0.01$, $***p<0.001$ vs. sham group. $n=5$–6.

The ER is necessary for the folding of all secreted and membrane proteins, and insults that impair its function induce a pathological state known as ER stress.[25] ER stress responses have long been implicated in neurodegeneration and cognitive dysfunction.[25–28] ER stress has been implicated in the secondary injury response in spinal cord tissue after traumam[31,62] but its induction at remote regions has not been reported. Our data show that an increased ER stress response in certain brain regions correlates with injury severity after thoracic SCI. There is substantial evidence to indicate that ER stress is linked to inflammation through several intersecting cellular pathways, particularly pro-inflammatory cytokines and reactive oxygen species.[27,63,64] Protein folding is an energy-demanding process that occurs in oxidizing conditions.[63] Many neurodegenerative diseases include inflammation and ER stress impacts inflammation.[65] Previous *in vitro* studies indicate that oligodendrocytes exposed to inflammatory proteins IFN-γ exhibit features of ER stress,[66] representing yet another link between ER stress and neuroinflammation. Previously, we and others[18,19,21,41] have shown significant elevation of pro-inflammatory cytokines in the hippocampi after SCI, including tumor necrosis factor (TNF)-α, interleukin (IL) 1-α, inducible nitric oxide synthase, CCL2/3. Thus, SCI-mediated chronic neuroinflammatory response in the brain may contribute to ER stress. Co-localization between GRP78, a marker of ER stress, and an immature neuronal marker also is greater after moderate or severe injury. Therefore, chronic activation of ER stress in the brain, as well as in newly-generated immature neurons in the hippocampal SGZ, may contribute to reduced neuronal survival and neurogenesis associated with impaired cognition and depression after SCI.

It is well known that chronic inflammation occurs in pain regulatory areas, such as brainstem and thalamus, after SCI, with posttraumatic hyperesthesia associated with plasticity or electrophysiological alterations.[53,67] Felix and colleagues reported an acute inflammatory response in the dorsal vagal complex, the subventricular zone, and subgranular zone of the hippocampal DG after rat cervical SCI.[36] Chemokines CCL2/CCL3 are chronically expressed not only in thalamus, but also in hippocampus (CA3 and DG sub-regions), and periaqueductal gray matter after severe SCI.[41] Our recent autoradiography studies[19] in rats after SCI, using a new TSPO ligand [^{125}I] IodoDPA-713, found that all brain regions examined (including cortex, thalamus, hippocampus, cerebellum, caudate/putamen) showed significantly elevated [^{125}I] IodoDPA-713 binding, indicating increased brain inflammation. These data complemented microscopy findings showing chronic microglial activation in the brain after SCI.[18,19] Stereological analysis in the present study detected no changes in total numbers of Iba-1^{+} microglia in either cerebral cortex or hippocampus across injury groups. BrdU-labeled microglia and astrocytes also showed no changes. Consistent with our previous finding,[18,19] reactive microglial phenotypes predominate chronically in the brain after moderate/severe SCI in mice.

It has been reported that inflammation influences several steps of adult neurogenesis, including the initial stages (i.e., proliferation, survival and neuronal fate determination) and later stages (i.e., synaptic assembly, stability, and transmission) of neurogenesis.[68] Adult new-born neurons are susceptible to brain inflammation.[38,39] Anti-inflammatory treatments prevent chronic brain inflammation–mediated decreased neurogenesis.[68–70] Alterations of the number and/or morphology of microglial cells, as well as the up-regulation of inflammatory cytokines, such as IL-1α, IL-6, TNFα, have been implicated in cognitive and behavioral changes observed in depressed subjects.[71] Consistent with these studies, we observe chronic inflammatory reactions in distant brain areas after SCI that

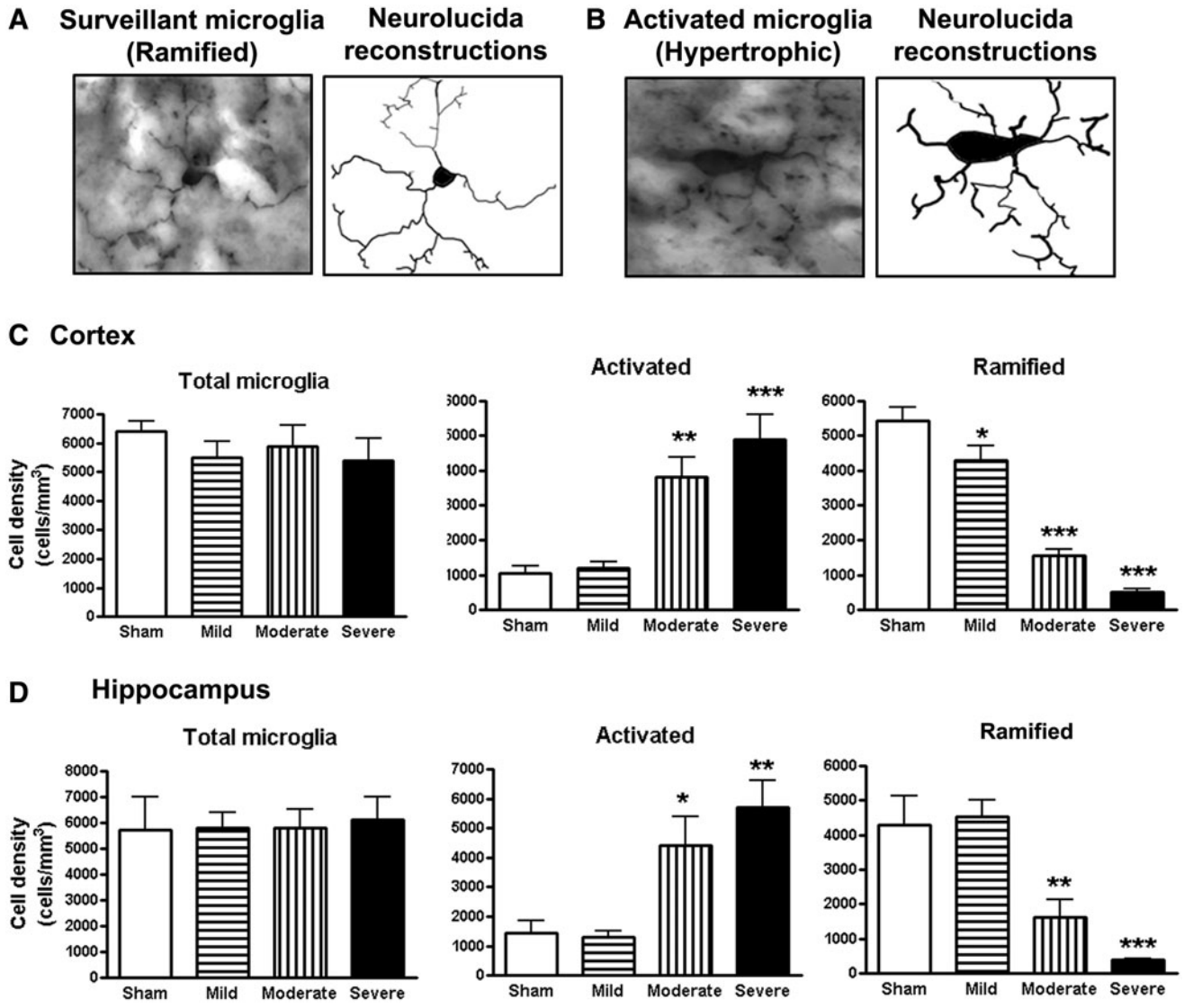

FIG. 8. Chronic spinal cord injury (SCI) increased activated microglial phenotypes in the brain at 16 weeks post-lesion. (**A** and **B**) Representative Iba-1 immunohistochemistry images displaying surveillant (ramified morphology) or activated (hypertrophic morphology) microglial phenotypes and the corresponding Neurolucida reconstructions. (**C** and **D**) Unbiased stereological quantitative assessment in the cortex (C) and hippocampus (D) revealed significant increased numbers of activated microglia displaying a hypertrophic cellular morphology and reduced numbers of surveillant microglia displaying the ramified cellular morphology in moderate/severe SCI mice, compared with sham mice. No significant differences were observed in the number of total microglia across the groups. $*p<0.05$, $**p<0.01$, $***p<0.001$, SCI vs. sham groups, $n=5$–6.

are associated with cognitive dysfunction and depressive-like behavior. However, the mechanisms underlying SCI-mediated microglial activation in the brain remain unknown. Neuronal cysteine-cysteine chemokine ligand 21 (CCL21) is synthesized by damaged neurons; following packaging in vesicles and transport, it reaches presynaptic sites, where it is released to activate microglia at sites distant from the primary lesion.[72–75] Spinal cord contusion injury at T9 increases CCL21 signal in excitatory neurons of the dorsal horn and in spinal parenchyma at both the T9 and L4 spinal segments.[54] Distal release of CCL21 produced following SCI by injured neurons at the trauma site has been proposed as a molecular mechanism that triggers microglial activation at spinal segments far from the site of injury, and in the thalamus in association with pain phenomena.[49,53] However, CCL21 changes appear to extend beyond these centers and impact other regions. We have shown that increased CCL21 signal in various brain regions are associated with microglial activation in these areas related to chronic neuronal cell loss after SCI.[19] Therefore, SCI-induced accumulation of CCL21 in key regions of the brain after SCI may contribute to microglial activation and related neuropsychiatric changes.

In the present study, mild SCI also induces significant increases in total number of $GRP78^+$ cells and CCL21 immunoreactivity in several important brain sub-regions, suggesting ER stress or neuroinflammatory response in the brain. The levels of ER stress will influence the outcome of the cellular response.[76] When ER stress is mild, the cell can recover and/or adapt. However, when ER stress is prolonged or too severe, these mechanisms fail to restore proteostasis leading to cell death.[77–79] This may explain that mild injury did not affect neuronal survival, as well as total number of activated microglia in the brain. ER stress significantly increases in an injury

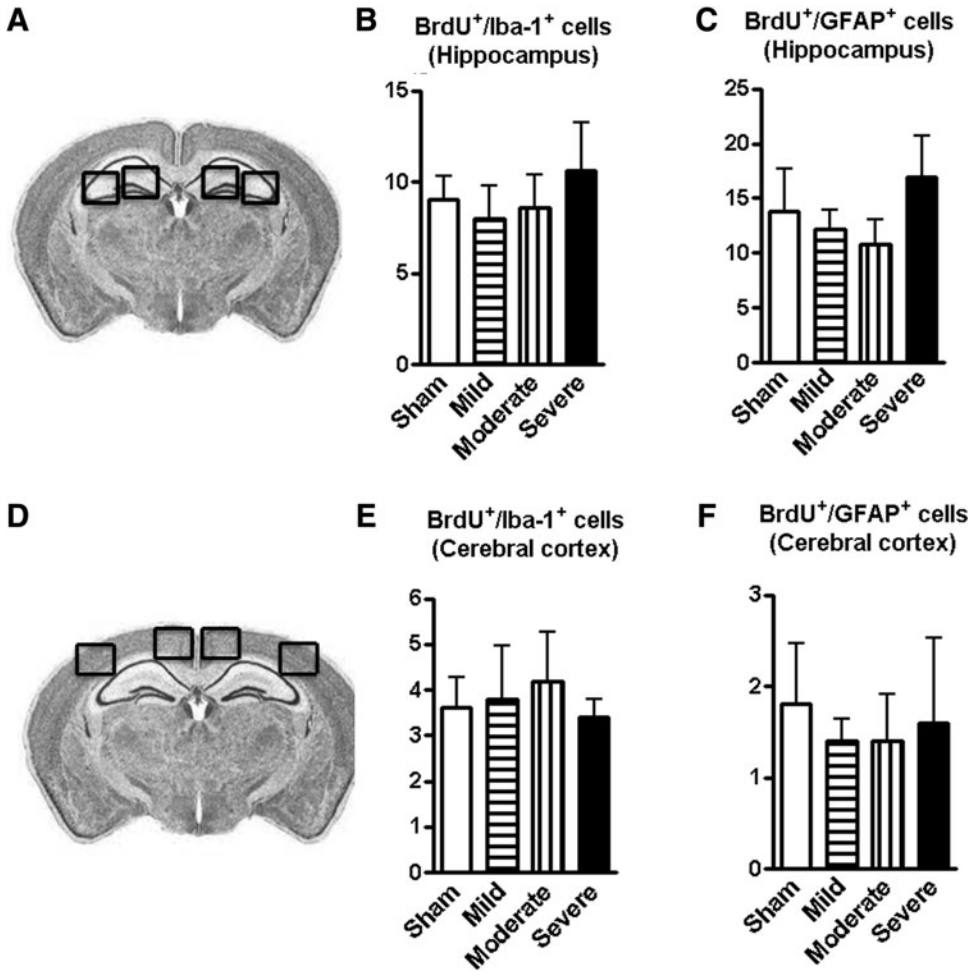

FIG. 9. Spinal cord injury (SCI) does not affect gliogenesis in the hippocampus and cerebral cortex. (**A** and **B**) Illustration of the hippocampal and cerebral cortical anatomical regions used for image analysis. (**C–F**) Numbers of co-localized bromo-deoxyuridine (BrdU)+/Iba-1+ and BrdU+/ glial fibrillary acidic protein + cells in the hippocampus and cortex did not change among all of SCI groups. $n = 5–6$.

severity–dependent manner in the hippocampus and thalamus. However, in the same samples, no significant differences were observed in the CCL21 expression across the injured groups. These findings suggest that these pathways demonstrate differential sensitivity to injury severity.

Assessments of neuronal cell death in the brain after SCI have been focused acutely on the motor cortex and are controversial, with conclusions ranging from no cell death to extensive retrograde degeneration. More recently, Felix and colleagues[36] assessed cells expressing active caspase-3, alone or in association with neuronal markers, in the forebrain after cervical SCI in rats. They were scarce under all conditions tested (control, 7, 15, 90 days post-injury), and no significant difference was observed between control and injured animals. In agreement with prior research,[36] we detected a few caspase-3^+ cells in brain sub-regions at 4 months after SCI (data not shown). The relatively rapid progress of cell death stages in any single neuron may explain the difficulty of directly detecting individual phases of this phenomenon. Moreover, there are no universally valid methods of detecting ongoing neuronal cell death, which reflects a heterogeneous process that includes various mechanisms. These issues are particularly relevant in models such as ours where the cell death is not acute but rather progressive over many weeks. Thus, we chose to focus on neuronal loss as a reflection of accumulated cell death over the duration of the study and to use a quantitative method based on unbiased stereology. This overall neuronal cell loss is arguably a better determinant of neurological deficits than any snapshot of precursor mechanisms. A limitation of the present approach is the difficulty in differentiating between the role of cell death in adult neurons versus neural progenitors/newly-formed cells. Thus, the diminished neuronal densities could be explained not only as cell death of mature neurons but also by an increased cell death of newly-formed cells. Future studies will need to examine these issues.

In summary, using a battery of established behavioral tests that are less dependent on motor function, we show that moderate/severe SCI leads to chronic impairments in cognitive functions and depression, and which are associated with impaired hippocampal neurogenesis. Moreover, we provide the first evidence that chronic activation of an ER stress response in the brain, as well as in newly-generated immature neurons in the hippocampal SGZ, may contribute to suppressed neuronal survival and neurogenesis. Finally, we show that the potent microglial activator CCL21 is elevated in the brain sites after SCI in association with increased microglial activation and suggest that this chemokine

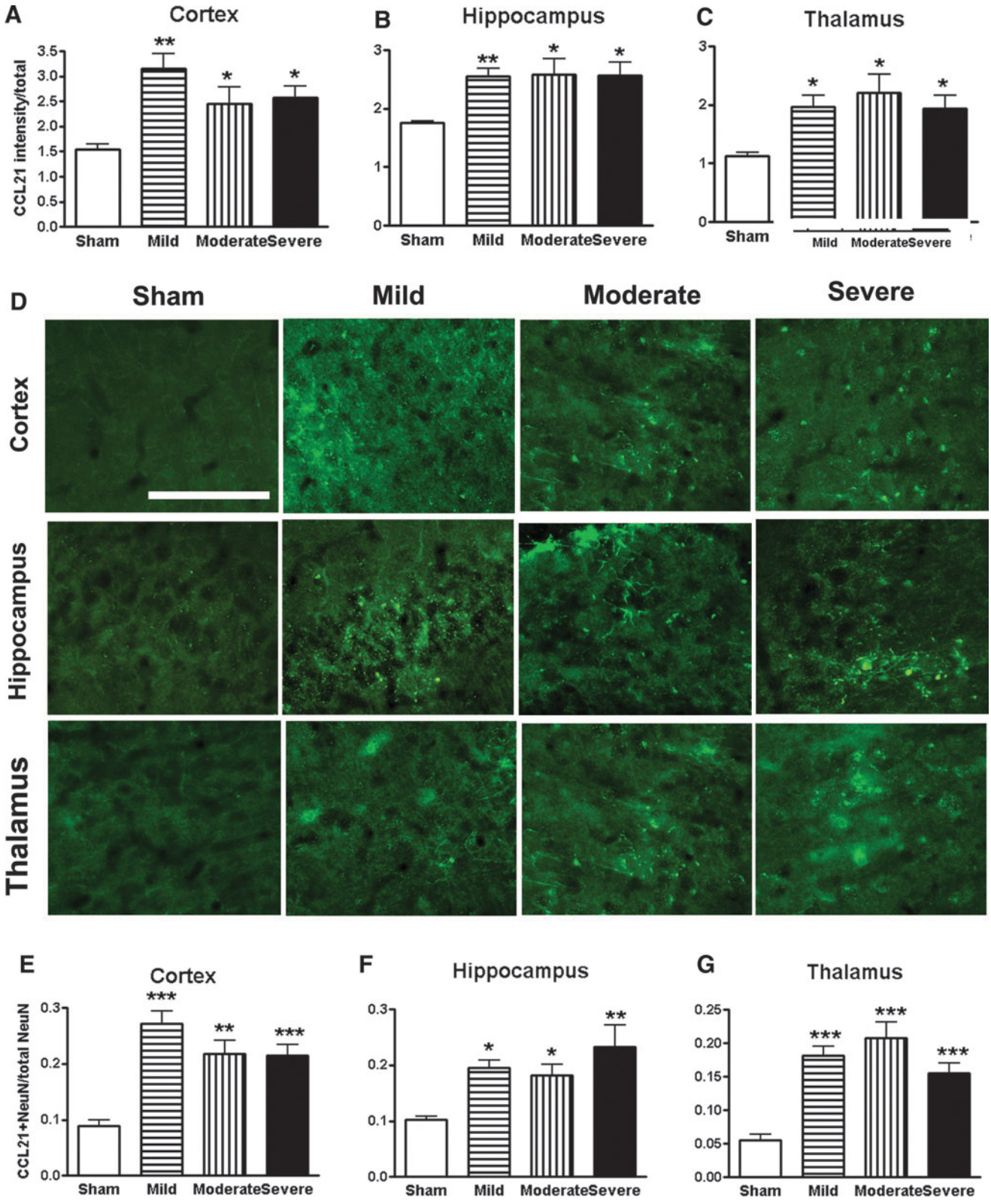

FIG. 10. Spinal cord injury (SCI) triggers CCL21 accumulation in the brain regions at 16 weeks post-injury. (**A–C**) Quantification of CCL21 immunointensity showed significantly increased in the cortex, hippocampus, and thalamus in all SCI groups. **(D)** Representative images of immunohistochemistry staining for CCL21 in the key brain regions from sham, mild, moderate, and severe SCI animals. **(E–G)** The proportion of CCL21+/NeuN+ double-labeling cells in total number of neurons was significantly increased in SCI groups. Scale bar is 50 μm. *$p<0.05$, **$p<0.01$, ***$p<0.001$ vs. sham group. $n=5$–6. Color image is available online at www.liebertpub.com/neu

may subserve a pathophysiological role in cognitive changes and depression after SCI.

Acknowledgments

We thank Shuxin Zhao, Craig Remenapp, and Xiya Zhu for expert technical support. This work was supported in part by National Institutes of Health Grants R01 NR013601 (AIF), a pilot project in P30 NR014129 (JW), Craig H. Neilsen Foundation senior grant 240442 (AIF), and startup funds from the Department of Anesthesiology and Center for Shock, Trauma and Anesthesiology Research (STAR), University of Maryland School of Medicine, Baltimore, MD (JW).

JW and AIF conceived research; JW designed research; ZZ, JW, AK, and DJL performed research; ZZ, JW, AK, and MML analyzed data; JW, BAS and AIF wrote the paper.

Author Disclosure Statement

No competing financial interests exist.

References

1. Davidoff, G.N., Roth, E.J., and Richards, J.S. (1992). Cognitive deficits in spinal cord injury: epidemiology and outcome. Arch. Phys. Med. Rehabil. 73, 275–284.
2. Jegede, A.B., Rosado-Rivera, D., Bauman, W.A., Cardozo, C.P., Sano, M., Moyer, J.M., Brooks, M., and Wecht, J.M. (2010). Cognitive performance in hypotensive persons with spinal cord injury. Clin. Auton. Res. 20, 3–9.
3. Lazzaro, I., Tran, Y., Wijesuriya, N., and Craig, A. (2013). Central correlates of impaired information processing in people with spinal cord injury. J. Clin. Neurophysiol. 30, 59–65.
4. Dowler, R.N., Harrington, D.L., Haaland, K.Y., Swanda, R.M., Fee, F., and Fiedler, K. (1997). Profiles of cognitive functioning in chronic spinal cord injury and the role of moderating variables. J. Int. Neuropsychol. Soc. 3, 464–472.
5. Jensen, M.P., Kuehn, C.M., Amtmann, D., and Cardenas, D.D. (2007). Symptom burden in persons with spinal cord injury. Arch. Phys. Med. Rehabil. 88, 638–645.
6. Roth, E., Davidoff, G., Thomas, P., Doljanac, R., Dijkers, M., Berent, S., Morris, J., and Yarkony, G. (1989). A controlled study of neuropsychological deficits in acute spinal cord injury patients. Paraplegia 27, 480–489.
7. Richards, J.S., Brown, L., Hagglund, K., Bua, G., and Reeder, K. (1988). Spinal cord injury and concomitant traumatic brain injury. Results of a longitudinal investigation. Am. J. Phys. Med. Rehabil. 67, 211–216.
8. Umlauf, R.L. (1992). Psychological interventions for chronic pain following spinal cord injury. Clin. J. Pain 8, 111–118.
9. Wecht, J.M. and Bauman, W.A. (2013). Decentralized cardiovascular autonomic control and cognitive deficits in persons with spinal cord injury. J. Spinal Cord Med. 36, 74–81.
10. Arango-Lasprilla, J.C., Ketchum, J.M., Starkweather, A., Nicholls, E., and Wilk, A.R. (2011). Factors predicting depression among persons with spinal cord injury 1 to 5 years post injury. NeuroRehabilitation 29, 9–21.
11. Kessler, R.C., Petukhova, M., Sampson, N.A., Zaslavsky, A.M., and Wittchen, H.U. (2012). Twelve-month and lifetime prevalence and lifetime morbid risk of anxiety and mood disorders in the United States. Int. J. Methods Psychiatr. Res. 21, 169–184.
12. Fullerton, D.T., Harvey, R.F., Klein, M.H., and Howell, T. (1981). Psychiatric disorders in patients with spinal cord injuries. Arch. Gen. Psychiatry 38, 1369–1371.
13. Migliorini, C.E., New, P.W., and Tonge, B.J. (2009). Comparison of depression, anxiety and stress in persons with traumatic and non-traumatic post-acute spinal cord injury. Spinal Cord 47, 783–788.
14. Bombardier, C.H., Fann, J.R., Tate, D.G., Richards, J.S., Wilson, C.S., Warren, A.M., Temkin, N.R., and Heinemann, A.W.; PRISMS Investigators. (2012). An exploration of modifiable risk factors for depression after spinal cord injury: which factors should we target? Arch. Phys. Med. Rehabil. 93, 775–781.
15. Krueger, H., Noonan, V.K., Williams, D., Trenaman, L.M., and Rivers, C.S. (2013). The influence of depression on physical complications in spinal cord injury: behavioral mechanisms and health-care implications. Spinal Cord 51, 260–266.
16. Hartkopp, A., Bronnum-Hansen, H., Seidenschnur, A.M., and Biering-Sorensen, F. (1998). Suicide in a spinal cord injured population: its relation to functional status. Arch. Phys. Med. Rehabil.79, 1356–1361.
17. Zhang, B., Huang, Y., Su, Z., Wang, S., Wang, S., Wang, J., Wang, A., and Lai, X. (2011). Neurological, functional, and biomechanical characteristics after high-velocity behind armor blunt trauma of the spine. J. Trauma 71, 1680–1688.
18. Wu, J., Zhao, Z., Sabirzhanov, B., Stoica, B.A., Kumar, A., Luo, T., Skovira, J., and Faden, A.I. (2014). Spinal cord injury causes brain inflammation associated with cognitive and affective changes: role of cell cycle pathways. J. Neurosci. 34, 10989–11006.
19. Wu, J., Stoica, B.A., Luo, T., Sabirzhanov, B., Zhao, Z., Guanciale, K., Nayar, S.K., Foss, C.A., Pomper, M.G., and Faden, A.I. (2014). Isolated spinal cord contusion in rats induces chronic brain neuroinflammation, neurodegeneration, and cognitive impairment: involvement of cell cycle activation. Cell Cycle 13.
20. Luedtke, K., Bouchard, S.M., Woller, S.A., Funk, M.K., Aceves, M., and Hook, M.A. (2014). Assessment of depression in a rodent model of spinal cord injury. J. Neurotrauma 31, 1107–1121.
21. Maldonado-Bouchard, S., Peters, K., Woller, S.A., Madahian, B., Faghihi, U., Patel, S., Bake, S., and Hook, M.A. (2015). Inflammation is increased with anxiety- and depression-like signs in a rat model of spinal cord injury. Brain Behav. Immun. 51, 176–195.
22. Sitia, R. and Braakman, I. (2003). Quality control in the endoplasmic reticulum protein factory. Nature 426, 891–894.
23. Fu, S., Watkins, S.M., and Hotamisligil, G.S. (2012). The role of endoplasmic reticulum in hepatic lipid homeostasis and stress signaling. Cell Metab. 15, 623–634.
24. Wang, M., Ye, R., Barron, E., Baumeister, P., Mao, C., Luo, S., Fu, Y., Luo, B., Dubeau, L., Hinton, D.R., and Lee, A.S. (2010). Essential role of the unfolded protein response regulator GRP78/BiP in protection from neuronal apoptosis. Cell Death Differ. 17, 488–498.
25. Roussel, B.D., Kruppa, A.J., Miranda, E., Crowther, D.C., Lomas, D.A., and Marciniak, S.J. (2013). Endoplasmic reticulum dysfunction in neurological disease. Lancet Neurol. 12, 105–118.
26. Hossain, M.M., DiCicco-Bloom, E., and Richardson, J.R. (2015). Hippocampal ER stress and learning deficits following repeated pyrethroid exposure. Toxicol. Sci. 143, 220–228.
27. Hotamisligil, G.S. (2010). Endoplasmic reticulum stress and the inflammatory basis of metabolic disease. Cell 140, 900–917.
28. Salminen, A., Kauppinen, A., Suuronen, T., Kaarniranta, K., and Ojala, J. (2009). ER stress in Alzheimer's disease: a novel neuronal trigger for inflammation and Alzheimer's pathology. J. Neuroinflammation 6, 41.
29. Valenzuela, V., Collyer, E., Armentano, D., Parsons, G.B., Court, F.A., and Hetz, C. (2012). Activation of the unfolded protein response enhances motor recovery after spinal cord injury. Cell Death Dis. 3, e272.
30. Penas, C., Verdu, E., Asensio-Pinilla, E., Guzman-Lenis, M.S., Herrando-Grabulosa, M., Navarro, X., and Casas, C. (2011). Valproate reduces CHOP levels and preserves oligodendrocytes and axons after spinal cord injury. Neuroscience 178, 33–44.
31. Liu, S., Sarkar, C., Dinizo, M., Faden, A.I., Koh, E.Y., Lipinski, M.M., and Wu, J. (2015). Disrupted autophagy after spinal cord injury is associated with ER stress and neuronal cell death. Cell Death Dis. 6, e1582.
32. Kee, N., Teixeira, C.M., Wang, A.H., and Frankland, P.W. (2007). Preferential incorporation of adult-generated granule cells into spatial memory networks in the dentate gyrus. Nat. Neurosci. 10, 355–362.
33. Gu, Y., Arruda-Carvalho, M., Wang, J., Janoschka, S.R., Josselyn, S.A., Frankland, P.W., and Ge, S. (2012). Optical controlling reveals time-dependent roles for adult-born dentate granule cells. Nat. Neurosci. 15, 1700–1706.
34. Rotheneichner, P., Lange, S., O'Sullivan, A., Marschallinger, J., Zaunmair, P., Geretsegger, C., Aigner, L., and Couillard-Despres, S. (2014). Hippocampal neurogenesis and antidepressive therapy: shocking relations. Neural Plasticity 2014, 723915.
35. Dimitrov, E.L., Tsuda, M.C., Cameron, H.A., and Usdin, T.B. (2014). Anxiety- and depression-like behavior and impaired neurogenesis

evoked by peripheral neuropathy persist following resolution of prolonged tactile hypersensitivity. J. Neurosci. 34, 12304–12312.
36. Felix, M.S., Popa, N., Djelloul, M., Boucraut, J., Gauthier, P., Bauer, S., and Matarazzo, V.A. (2012). Alteration of forebrain neurogenesis after cervical spinal cord injury in the adult rat. Front. Neurosci. 6, 45.
37. Mutso, A.A., Radzicki, D., Baliki, M.N., Huang, L., Banisadr, G., Centeno, M.V., Radulovic, J., Martina, M., Miller, R.J., and Apkarian, A.V. (2012). Abnormalities in hippocampal functioning with persistent pain. J. Neurosci. 32, 5747–5756.
38. Chugh, D., Nilsson, P., Afjei, S.A., Bakochi, A., and Ekdahl, C.T. (2013). Brain inflammation induces post-synaptic changes during early synapse formation in adult-born hippocampal neurons. Exp. Neurol. 250, 176–188.
39. Jakubs, K., Bonde, S., Iosif, R.E., Ekdahl, C.T., Kokaia, Z., Kokaia, M., and Lindvall, O. (2008). Inflammation regulates functional integration of neurons born in adult brain. J. Neurosci. 28, 12477–12488.
40. Gomez-Pinilla, F., Ying, Z., and Zhuang, Y. (2012). Brain and spinal cord interaction: protective effects of exercise prior to spinal cord injury. PLoS One 7, e32298.
41. Knerlich-Lukoschus, F., Noack, M., von der Ropp-Brenner, B., Lucius, R., Mehdorn, H.M., and Held-Feindt, J. (2011). Spinal cord injuries induce changes in CB1 cannabinoid receptor and C-C chemokine expression in brain areas underlying circuitry of chronic pain conditions. J. Neurotrauma 28, 619–634.
42. Wu, J., Renn, C.L., Faden, A.I., and Dorsey, S.G. (2013). TrkB.T1 contributes to neuropathic pain after spinal cord injury through regulation of cell cycle pathways. J. Neurosci. 33, 12447–12463.
43. Basso, D.M., Fisher, L.C., Anderson, A.J., Jakeman, L.B., McTigue, D.M., and Popovich, P.G. (2006). Basso Mouse Scale for locomotion detects differences in recovery after spinal cord injury in five common mouse strains. J. Neurotrauma 23, 635–659.
44. Zhao, Z., Loane, D.J., Murray, M.G. 2nd, Stoica, B.A., and Faden, A.I. (2012). Comparing the predictive value of multiple cognitive, affective, and motor tasks after rodent traumatic brain injury. J. Neurotrauma 29, 2475–2489.
45. Wang, S.H., Zhang, Z.J., Guo, Y.J., Zhou, H., Teng, G.J., and Chen, B.A. (2009). Anhedonia and activity deficits in rats: impact of post-stroke depression. J. Psychopharmacol. 23, 295–304.
46. Zhou, W., Dantzer, R., Budac, D.P., Walker, A.K., Mao-Ying, Q.L., Lee, A.W., Heijnen, C.J., and Kavelaars, A. (2015). Peripheral indoleamine 2,3-dioxygenase 1 is required for comorbid depression-like behavior but does not contribute to neuropathic pain in mice. Brain Behav. Immun. 46, 147–153.
47. Walker, A.K., Budac, D.P., Bisulco, S., Lee, A.W., Smith, R.A., Beenders, B., Kelley, K.W., and Dantzer, R. (2013). NMDA receptor blockade by ketamine abrogates lipopolysaccharide-induced depressive-like behavior in C57BL/6J mice. Neuropsychopharmacology 38, 1609–1616.
48. Sarkar, C., Zhao, Z., Aungst, S., Sabirzhanov, B., Faden, A.I., and Lipinski, M.M. (2014). Impaired autophagy flux is associated with neuronal cell death after traumatic brain injury. Autophagy 10, 2208–2222.
49. Wu, J., Raver, C., Piao, C., Keller, A., and Faden, A.I. (2013). Cell cycle activation contributes to increased neuronal activity in the posterior thalamic nucleus and associated chronic hyperesthesia after rat spinal cord contusion. Neurotherapeutics 10, 520–538.
50. Lee, H.J., Wu, J., Chung, J., and Wrathall, J.R. (2013). SOX2 expression is upregulated in adult spinal cord after contusion injury in both oligodendrocyte lineage and ependymal cells. J. Neurosci. Res. 91, 196–210.
51. Soltys, Z., Ziaja, M., Pawlinski, R., Setkowicz, Z., and Janeczko, K. (2001). Morphology of reactive microglia in the injured cerebral cortex. Fractal analysis and complementary quantitative methods. J. Neurosci. Res. 63, 90–97.
52. Byrnes, K.R., Loane, D.J., Stoica, B.A., Zhang, J., and Faden, A.I. (2012). Delayed mGluR5 activation limits neuroinflammation and neurodegeneration after traumatic brain injury. J. Neuroinflammation 9, 43.
53. Zhao, P., Waxman, S.G., and Hains, B.C. (2007). Modulation of thalamic nociceptive processing after spinal cord injury through remote activation of thalamic microglia by cysteine cysteine chemokine ligand 21. J. Neurosci. 27, 8893–8902.
54. Hulsebosch, C.E., Hains, B.C., Crown, E.D., and Carlton, S.M. (2009). Mechanisms of chronic central neuropathic pain after spinal cord injury. Brain Res. Rev. 60, 202–213.
55. Wu, J., Sabirzhanov, B., Stoica, B.A., Lipinski, M.M., Zhao, Z., Zhao, S., Ward, N., Yang, D., and Faden, A.I. (2015). Ablation of the transcription factors E2F1-2 limits neuroinflammation and associated neurological deficits after contusive spinal cord injury. Cell Cycle 14, 3698–3712.
56. Wu, J., Zhao, Z., Zhu, X., Renn, C.L., Dorsey, S.G., and Faden, A.I. (2016). Cell cycle inhibition limits development and maintenance of neuropathic pain following spinal cord injury. Pain 157, 488–503.
57. Eisch, A.J. and Petrik, D. (2012). Depression and hippocampal neurogenesis: a road to remission? Science 338, 72–75.
58. Santarelli, L., Saxe, M., Gross, C., Surget, A., Battaglia, F., Dulawa, S., Weisstaub, N., Lee, J., Duman, R., Arancio, O., Belzung, C., and Hen, R. (2003). Requirement of hippocampal neurogenesis for the behavioral effects of antidepressants. Science 301, 805–809.
59. Sahay, A. and Hen, R. (2007). Adult hippocampal neurogenesis in depression. Nat Neurosci 10, 1110–1115.
60. Malberg, J.E., Eisch, A.J., Nestler, E.J., and Duman, R.S. (2000). Chronic antidepressant treatment increases neurogenesis in adult rat hippocampus. J. Neurosci. 20, 9104–9110.
61. Franz, S., Ciatipis, M., Pfeifer, K., Kierdorf, B., Sandner, B., Bogdahn, U., Blesch, A., Winner, B., and Weidner, N. (2014). Thoracic rat spinal cord contusion injury induces remote spinal gliogenesis but not neurogenesis or gliogenesis in the brain. PLoS One 9, e102896.
62. Ohri, S.S., Hetman, M., and Whittemore, S.R. (2013). Restoring endoplasmic reticulum homeostasis improves functional recovery after spinal cord injury. Neurobiol. Dis. 58, 29–37.
63. Tu, B.P. and Weissman, J.S. (2002). The FAD- and O(2)-dependent reaction cycle of Ero1-mediated oxidative protein folding in the endoplasmic reticulum. Mol. Cell 10, 983–994.
64. Deslauriers, A.M., Afkhami-Goli, A., Paul, A.M., Bhat, R.K., Acharjee, S., Ellestad, K.K., Noorbakhsh, F., Michalak, M., and Power, C. (2011). Neuroinflammation and endoplasmic reticulum stress are coregulated by crocin to prevent demyelination and neurodegeneration. J. Immunol. 187, 4788–4799.
65. Zhang, K. and Kaufman, R.J. (2008). From endoplasmic-reticulum stress to the inflammatory response. Nature 454, 455–462.
66. Lin, W., Harding, H.P., Ron, D., and Popko, B. (2005). Endoplasmic reticulum stress modulates the response of myelinating oligodendrocytes to the immune cytokine interferon-gamma. J. Cell Biol. 169, 603–612.
67. Hains, B.C. and Waxman, S.G. (2006). Activated microglia contribute to the maintenance of chronic pain after spinal cord injury. J. Neurosci. 26, 4308–4317.
68. Ekdahl, C.T. (2012). Microglial activation - tuning and pruning adult neurogenesis. Front. Pharmacol. 3, 41.
69. Monje, M.L., Toda, H., and Palmer, T.D. (2003). Inflammatory blockade restores adult hippocampal neurogenesis. Science 302, 1760–1765.
70. Ekdahl, C.T., Claasen, J.H., Bonde, S., Kokaia, Z., and Lindvall, O. (2003). Inflammation is detrimental for neurogenesis in adult brain. Proc. Natl. Acad. Sci. U. S. A. 100, 13632–13637.
71. Reus, G.Z., Fries, G.R., Stertz, L., Badawy, M., Passos, I.C., Barichello, T., Kapczinski, F., and Quevedo, J. (2015). The role of inflammation and microglial activation in the pathophysiology of psychiatric disorders. Neuroscience 300, 141–154.
72. de Jong, E.K., Dijkstra, I.M., Hensens, M., Brouwer, N., van Amerongen, M., Liem, R.S., Boddeke, H.W., and Biber, K. (2005). Vesicle-mediated transport and release of CCL21 in endangered neurons: a possible explanation for microglia activation remote from a primary lesion. J. Neurosci. 25, 7548–7557.
73. Biber, K., Tsuda, M., Tozaki-Saitoh, H., Tsukamoto, K., Toyomitsu, E., Masuda, T., Boddeke, H., and Inoue, K. (2011). Neuronal CCL21 up-regulates microglia P2X4 expression and initiates neuropathic pain development. EMBO J. 30, 1864–1873.
74. de Haas, A.H., van Weering, H.R., de Jong, E.K., Boddeke, H.W., and Biber, K.P. (2007). Neuronal chemokines: versatile messengers in central nervous system cell interaction. Mol. Neurobiol. 36, 137–151.
75. de Jong, E.K., Vinet, J., Stanulovic, V.S., Meijer, M., Wesseling, E., Sjollema, K., Boddeke, H.W., and Biber, K. (2008). Expression, transport, and axonal sorting of neuronal CCL21 in large dense-core vesicles. FASEB J. 22, 4136–4145.
76. Tsang, K.Y., Chan, D., Bateman, J.F., and Cheah, K.S. (2010). In vivo cellular adaptation to ER stress: survival strategies with double-edged consequences. J. Cell Sci. 123, 2145–2154.

77. Decuypere, J.P., Monaco, G., Bultynck, G., Missiaen, L., De Smedt, H., and Parys, J.B. (2011). The IP(3) receptor-mitochondria connection in apoptosis and autophagy. Biochim. Biophys. Acta 1813, 1003–1013.
78. Deegan, S., Saveljeva, S., Gorman, A.M., and Samali, A. (2013). Stress-induced self-cannibalism: on the regulation of autophagy by endoplasmic reticulum stress. Cell. Mol. Life Sci. 70, 2425–2441.
79. Kim, I., Xu, W., and Reed, J.C. (2008). Cell death and endoplasmic reticulum stress: disease relevance and therapeutic opportunities. Nat. Rev. Drug Discov. 7, 1013–1030.

Address correspondence to:
Junfang Wu, PhD
Department of Anesthesiology and Center
for Shock, Trauma, and Anesthesiology Research (STAR)
University of Maryland
School of Medicine
655 West Baltimore Street, #6-011
Baltimore, MD 21201

E-mail address: jwu@anes.umm.edu